Adaptive Mesh Refinement based Simulation of a Three-dimensional Methane-Oxygen Rotating Detonation Rocket Engine

Megan Powers, Shivank Sharma, Venkat Raman
University of Michigan
Ann Arbor, MI, USA

1 Introduction

Pressure gain devices have been studied since the 1960s [1], but their popularity has increased in recent years due to evolving design requirements. The rotating detonation rocket engine (RDRE), which employs detonation-based combustion, offers a theoretical 20% efficiency gain over deflagration engines [2]. For safety, fuel and oxidizer are injected separately, and axially traveling detonation waves provide continuous thrust, unlike pulse detonation engines (PDEs). However, the non-premixed nature of RDREs leads to parasitic deflagration [3], causing premature burning that weakens the detonation wave. Blockage and reverse flow into injectors reduce mixing time in the chamber, resulting in incomplete mixing and detonation waves that fail to achieve Chapman-Jouguet (CJ) speed or von Neumann pressure. This study leverages adaptive mesh refinement (AMR) in RDRE simulations to reduce computational costs, focusing on the effects of grid resolution on injector dynamics, combustion chamber behavior, and wave dynamics.

Grid resolution can have a major impact on the wave dynamics in an RDRE during transient and steady-state operation. The spatial resolution requirements for hydrocarbon/air mixtures have been shown to be greater than 100 μm [4]. Grid convergence studies have shown that the wave speed is highly dependent on the grid resolution [5]. As the grid resolution improves, the peak pressure following the detonation wave increases, resulting in an increase in wave velocity. In addition, the number of waves formed depends on the numerical methods used to handle transient wave collisions and the minimum grid resolution [5]. The Model Validation for Propulsion (MVP) workshop at the 2021 AIAA SciTech forum served as a platform to validate both experimental [6] and computational [7–11] efforts focused on AFRL's methane-oxygen RDRE. Building on the numerical study by Prakash et al. [9], which used the unstructured solver UMdetFOAM [12] to observe two co-rotating detonation waves in the channel, this work employs an in-house block-structured AMR solver [13] to target critical areas for refinement. This approach not only reduces computational costs, but also offers insight into how grid resolution influences overall wave dynamics.

2 Flow Configuration

The AFRL methane-oxygen RDRE geometry consists of 72 pairs of impinging fuel and oxidizer injectors with a 5 mm detonation channel. An area ratio of 0.1 is prescribed between the oxidizer injectors and the detonation annulus. The complete geometry and the cross-sectional schematic with primary dimensions are shown in Fig. 1. The flow conditions for this simulation are given in Table 1 which correspond to the baseline case for the MVP workshop. The boundary condition for maintaining

Correspondence to: powerm@umich.edu

a constant mass flow rate requires that the pressure in the plenums (p_{fuel} and p_{oxidizer}) be adjusted as required. Once the injectors are choked, the pressures in the fuel and oxidizer plenums stabilize near the initial conditions prescribed in Table 1, with adjustments occurring as detonation waves pass. In addition to the constant flow rate boundary condition, a zero-gradient pressure boundary condition is applied at the entrance of the plenums.

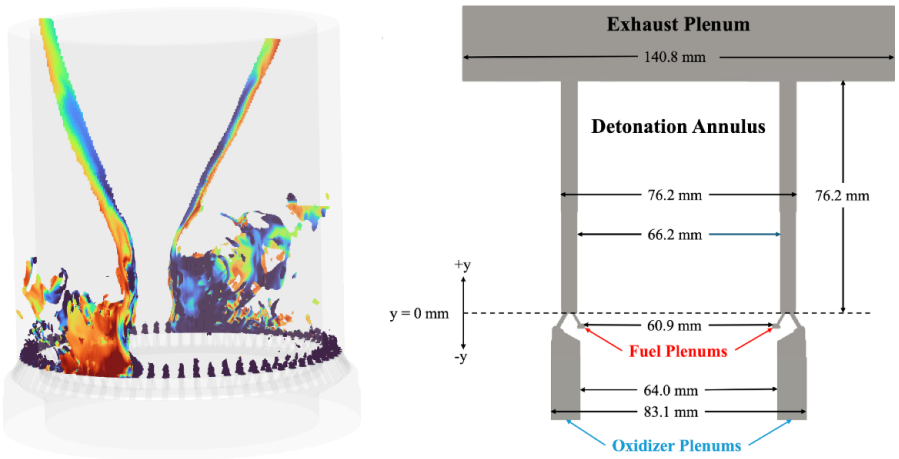

Figure 1: (Left) Full-scale geometry and (Right) cross-sectional schematic with primary dimensions.

Table 1: Flow Conditions

$\dot{m}_{\text{fuel}}$ [kg/s]	$\dot{m}_{\text{oxidizer}}$ [kg/s]	$\dot{m}_{\text{total}}$ [kg/s]	ϕ	p_{fuel} [MPa]	p_{oxidizer} [MPa]	T_{o} [K]	p_{back} [MPa]
0.06	0.207	0.267	1.15	1.31	1.20	300	0.1

The simulation begins by filling the domain with air and running without reactions until the detonation annulus is filled with a methane-oxygen mixture, which takes approximately 0.2 ms. Then, one kernel is placed in the detonation annulus and the flow is allowed to settle to a steady state, which takes approximately 1.0 ms. The resolution of the grid is set to 100 μm in the injectors and plenums, 200 μm in the lower half of the detonation chamber and 400 μm in the upper half of the detonation chamber. This resolution led to 70 million control volumes running on 2880 CPUs.

3 Numerical Methods

The governing equations for mass, momentum, energy, and species transport (refer to Equations 1–6 in [13]) are solved in a Cartesian coordinate system using a second-order finite-volume discretization method. Time integration is performed using a strong stability-preserving second-order Runge–Kutta scheme. The simulations utilize an in-house compressible flow solver [13] built on the AMReX library [14], which provides an AMR framework. A combination of the embedded boundary (EB) method [15, 16] and AMR-based local refinement is implemented to accurately capture geometric details. To mitigate the restrictive time step imposed by the small cut cells, a state redistribution approach [17] is adopted. The numerical methods, models, and approaches have been validated in several previous studies [18–20]. Detailed finite-rate chemistry is simulated using Cantera [21] with the FFCMy-12 mechanism [22] consisting of 13 species and 38 reactions; inert N_2 was added as the thirteenth species. Additional details and models can be found in [13] and [18], respectively.

4 Results and Discussion

Two co-rotating detonation waves were sustained after 1.0 ms, and the simulation continued for an additional one to two more wave cycles, roughly 0.2 ms. Two co-rotating detonation waves matched the experimental results [6]. Figure 2 shows a 2D unwrapped contour of temperature and pressure in the center of the detonation annulus. Fuel and oxidizer injection is shown in the low temperature regions. The fill height in the detonation chamber reached approximately 15 mm before the next detonation wave hit the reactants in the detonation annulus. The detonation and oblique shock structure separates the cold injector region from the post-detonation gas region. The shape of the detonation evolves over time between the two waves, and the acoustic and transverse waves affect the structure of both the main detonation and the oblique shock front, as shown in Fig. 2. The acoustic waves are being shed from the main detonation front and impact the shape of the following wave. In Fig. 2, parasitic combustion [3] can be seen as the top region where fresh reactants interact with post-detonation products before the detonation wave passes. This can reduce the overall efficiency of the RDRE.

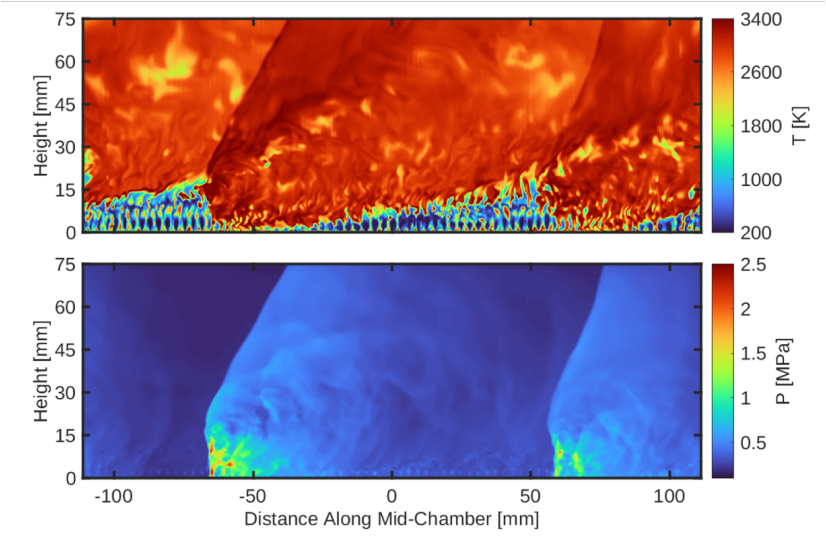

Figure 2: 2D projection of temperature contour (top) and pressure contour (bottom) at the radial midpoint of the channel.

The average pressure profile along the outer wall of the RDRE is shown in Fig. 3. Both this simulation and Prakash et al. [9] produced higher mean pressures than the experimental continuous tube attenuated pressure (CTAP) measurements. The peak pressure of this simulation occurs between 5-10 mm similar to Prakash et al. [9]. This suggests that the height of the detonation wave is between 5-10 mm. The drop in pressure after 10 mm corresponds to the oblique shock affixed to the detonation surface. The CTAP pressure measurements from the simulation range from 25-20% higher than the experimental values [6]. The percentage error between this simulation is in line with the other simulations done for this MVP geometry and initial condition [7–11]. The plan is to run higher grid resolution studies with longer time averaging to understand the impact on grid resolution on macroscopic properties.

Wave cycle statistics are averaged spatially over the detonation annulus and temporally over one injector pair across one- to two-wave cycles. Spatial averaging is performed on a single injector pair, while temporal averaging is performed at uniform time intervals. Figure 4 shows time-averaged mixture fraction, normalized heat release rate, and temperature. Detonations occur in slightly richer mixtures, propagating near the inner wall, where mixing is more uniform. Normalized heat release peaks 5 to 15 mm above injectors in this simulation, similar to Prakash et al. [9]. While the detonation wave travels closer to the inner wall, higher temperatures are seen closer to the outer wall.

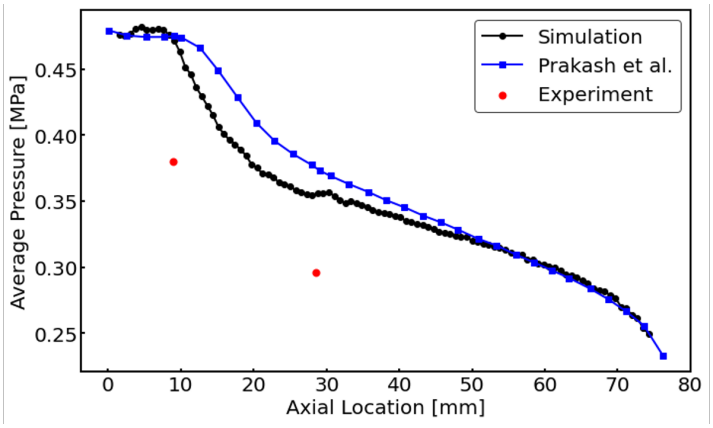

Figure 3: Average pressure on the outer wall from simulations and the experiment.

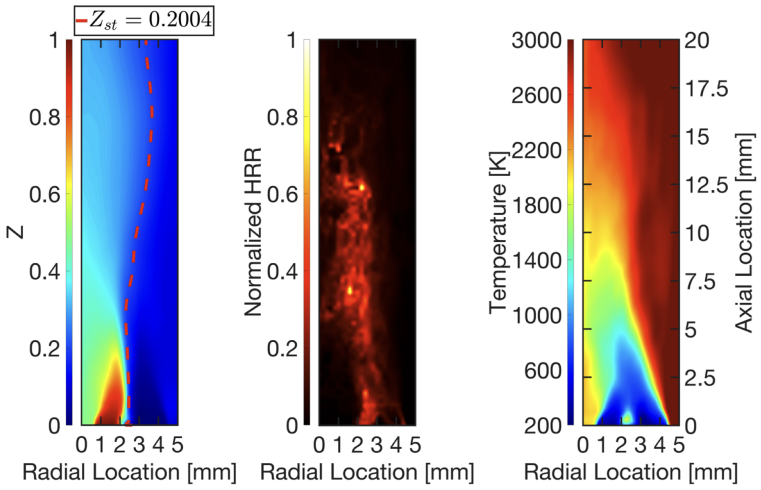

Figure 4: (Left) Mixture fraction, (middle) normalized heat release rate, and (right) temperature contours in the z-normal plane.

5 Conclusions

A high-fidelity simulation of a methane-oxygen RDRE was performed using AMR to target critical areas of the detonation front to understand the impact of wave dynamics. This simulation produced two co-rotating waves traveling at approximately 72% CJ speed with the current resolution. The time-averaged cross-section of the injectors revealed that the detonation wave was located closer to the inner wall. The heat release rate peaked between 5 and 15 mm above the injector location, and higher temperatures were observed on the outer wall. This work is still ongoing, and the goal is to conduct a grid resolution study comparing the macroscopic performance properties of the RDRE by introducing additional levels of refinement to track the detonation waves.

References

[1] J. Nicholls, R. E. Cullen, and K. Ragland, "Feasibility studies of a rotating detonation wave rocket motor." *Journal of Spacecraft and Rockets*, vol. 3, no. 6, pp. 893–898, 1966.

[2] I. J. Shaw, J. A. Kildare, M. J. Evans, A. Chinnici, C. A. Sparks, S. N. Rubaiyat, R. C. Chin, and P. R. Medwell, "A theoretical review of rotating detonation engines," in *Direct Numerical Simulations*, S. Rao, Ed. Rijeka: IntechOpen, 2019, ch. 7.

[3] F. Chacon and M. Gamba, "Study of parasitic combustion in an optically accessible continuous wave rotating detonation engine," in *AIAA scitech 2019 forum*, 2019, p. 0473.

[4] T. Lu, C. K. Law, and Y. Ju, "Some aspects of chemical kinetics in chapman-jouguet detonation: Induction length analysis," *Journal of Propulsion and Power*, vol. 19, no. 5, pp. 901–907, 2003.

[5] A. K. Hayashi, K. Shimomura, N. Tsuboi, K. Ozawa, N. H. Jourdaine, K. Ishii, E. Dzieminska, T. Obara, S. Maeda, and T. Mizukaki, "3d numerical study on flow field in disc-rde," in *AIAA Propulsion and Energy 2021 Forum*, 2021, p. 3665.

[6] J. W. Bennewitz, J. R. Burr, B. R. Bigler, R. F. Burke, A. Lemcherfi, T. Mundt, T. Rezzag, E. W. Plaehn, J. Sosa, I. V. Walters *et al.*, "Experimental validation of rotating detonation for rocket propulsion," *Scientific Reports*, vol. 13, no. 1, p. 14204, 2023.

[7] P. Pal, S. Demir, and S. Som, "Numerical analysis of combustion dynamics in a full-scale rotating detonation rocket engine using large eddy simulations," *Journal of Energy Resources Technology*, vol. 145, no. 2, p. 021702, 2023.

[8] P. Strakey and D. H. Ferguson, "Validation of a computational fluid dynamics model of a methane-oxygen rotating detonation engine," in *AIAA scitech 2022 forum*, 2022, p. 1113.

[9] S. Prakash, "Computational modeling of non-idealities in gaseous and multiphase detonating flows," Ph.D. dissertation, University of Michigan, 2022.

[10] K. A. Schau and J. C. Oefelein, "Numerical analysis of wave characteristics in a methane-oxygen rotating detonation engine," *AIAA Journal*, vol. 61, no. 1, pp. 97–111, 2023.

[11] M. Ross, J. R. Burr, and M. E. Harvazinski, "Relating high-fidelity rdre simulations to thermodynamic cycles, using fluid trajectories," in *AIAA SCITECH 2024 Forum*, 2024, p. 2036.

[12] *Detailed Chemical Kinetics Based Simulation of Detonation-Containing Flows*, ser. Turbo Expo: Power for Land, Sea, and Air, vol. Volume 4A: Combustion, Fuels, and Emissions, 06 2018.

[13] S. Sharma, R. Bielawski, O. Gibson, S. Zhang, V. Sharma, A. H. Rauch, J. Singh, S. Abisleiman, M. Ullman, S. Barwey, and V. Raman, "An amrex-based compressible reacting flow solver for high-speed reacting flows relevant to hypersonic propulsion," *arXiv preprint arXiv:2412.00900*, 2024.

[14] W. Zhang, A. Almgren, V. Beckner, J. Bell, J. Blaschke, C. Chan, M. Day, B. Friesen, K. Gott, D. Graves *et al.*, "Amrex: a framework for block-structured adaptive mesh refinement," *The Journal of Open Source Software*, vol. 4, no. 37, p. 1370, 2019.

[15] R. B. Pember, J. B. Bell, P. Colella, W. Y. Curtchfield, and M. L. Welcome, "An adaptive cartesian grid method for unsteady compressible flow in irregular regions," *Journal of Computational Physics*, vol. 120, no. 2, pp. 278–304, 1995.

[16] P. Colella, D. T. Graves, B. J. Keen, and D. Modiano, "A cartesian grid embedded boundary method for hyperbolic conservation laws," *Journal of Computational Physics*, vol. 211, no. 1, pp. 347–366, 2006.

[17] A. Giuliani, A. S. Almgren, J. B. Bell, M. J. Berger, M. H. de Frahan, and D. Rangarajan, "A weighted state redistribution algorithm for embedded boundary grids," *Journal of Computational Physics*, vol. 464, p. 111305, 2022.

[18] R. Bielawski, S. Barwey, S. Prakash, and V. Raman, "Highly-scalable gpu-accelerated compressible reacting flow solver for modeling high-speed flows," *Computers & Fluids*, vol. 265, p. 105972, 2023.

[19] T. Sato and V. Raman, "Detonation structure in ethylene/air-based non-premixed rotating detonation engine," *Journal of Propulsion and Power*, vol. 36, no. 5, pp. 752–762, 2020.

[20] S. Prakash, V. Raman, C. F. Lietz, W. A. Hargus Jr, and S. A. Schumaker, "Numerical simulation of a methane-oxygen rotating detonation rocket engine," *Proceedings of the Combustion Institute*, vol. 38, no. 3, pp. 3777–3786, 2021.

[21] D. G. Goodwin, R. L. Speth, H. K. Moffat, and B. W. Weber, "Cantera: An object-oriented software toolkit for chemical kinetics, thermodynamics, and transport processes," *Zenodo*, 2018.

[22] G. P. Smith, Y. Tao, and H. Wang, "Foundational fuel chemistry model version 1.0 (ffcm-1)," *epub, accessed July*, vol. 26, p. 2018, 2016.